ORIGINAL ARTICLE

Facile and sustainable modification for improving the adsorption ability of sugarcane bagasse towards cationic organic pollutants

Pengcheng Luan[1] · Jianming Liao[1] · Li Chen[1] · Yishan Kuang[1] · Xi Zhang[1] · Yuxiang Zhang[1] · Yikui Zhu[1] · Yonghong Dai[2] · Lihuan Mo[1] · Jun Li[1]

Abstract

Using low-cost agro-industrial wastes and by-products derived from lignocellulosic biomass for adsorption is considered to be an affordable and sustainable way to tackle the burning issue of cationic pollution in the water bodies, while its relatively low adsorption capability limits its large-scale application. In this study, a green, rapid, simple, and cheap method was developed by using ozone to improve the adsorption abilities of sugarcane bagasse (SB). The relationship between the chemical compositions and functional groups of SB after ozone modification and its adsorption abilities was studied. Results showed that ozone modification under very low ozone consumption (~ 1.5 wt%) could efficiently increase the pore volume, surface area, and carboxyl groups, change the chemical compositions of SB, and does not significantly change its morphology, thereby ensuring the good adsorption performance of SB and easy recycling from the water bodies. The maximum adsorption rate and equilibrium adsorption capacity of SB for positively charged methylene blue (MB) were increased about 33.3% and 11.3% than the original SB (MB concentration = 100 mg/L, SB concentration = 5 g/L, initial solution pH = 6, temperature = 30 °C). Besides, ozone-modified SB maintained its high adsorption capability even at a high NaCl concentration of 0.6 M and high pH of 9. For cationic polymer with high charge densities, the adsorption capacity of milled SB increased about 125.4%.

Keywords Sugarcane bagasse · Ozone modification · Cationic organic pollution · Biosorption

1 Introduction

Water bodies, including oceans, seas, and lakes, are of crucial importance not only to the global ecosystems but also to the nutrient supplies. Statistics show that more than 155 million tons of food are taken from the ocean every year, providing at least 20% of the total animal proteins for 3.1 billion people [1]. Besides, they are also important sources of amino acids, micronutrients, and vitamins and the only natural dietary source of n-3 polyunsaturated fatty acids, which are essential for the normal growth of young children [2]. However, due to the fast development of world industry and occasionally occurred pollution emergencies, water pollution has seriously damaged the ecological environment and thus adversely affected the food safety. Major water pollutants include chemicals and plastics. Among them, cationic organic pollutants, such as cationic dyes (Methyl Blue (MB), Cationic Orange G, Basic Red 29, etc.), are one of the main chemical pollutants, which have strong carcinogenic and mutagenic effects and can enter into the human consumers' bodies by the bioaccumulation, causing long-term toxic effects. [3] More importantly, in the water bodies, cationic organic pollutants have the features of long duration, wide spreading, and difficult to control. Therefore, effective removal of cationic organic pollutants in the water bodies is urgent and necessary.

Currently, the main strategies for the removal of cationic organic pollutants in the water bodies include physical (adsorption, membrane separation, etc.), chemical (oxidation, coagulation, etc.), and biological methods (aerobic and anaerobic treatment) or a combination of two or three above

Pengcheng Luan and Jianming Liao contributed equally to this paper.

✉ Jun Li
 ppjunli@scut.edu.cn

1 State Key Laboratory of Pulp and Paper Engineering, South China University of Technology, Guangzhou 510641, People's Republic of China

2 Guangxi Boguan Environmental Products Co. Ltd., Guangxi 547000, People's Republic of China

methods [4–6]. However, since most cationic organic pollutants have high chemical resistance due to their complex chemical structure and the complexity of components in wastewater (such as high salt content), most of the above methods are costly, poorly feasible, and have secondary pollution concerns.

Recently, adsorption by using low-cost lignocellulosic biomass, especially for the agro-industrial wastes and by-products, to remove the cationic organic pollutants from the water bodies is considered a promising technology because of its simple operation process and high feasibility [7]. Among those agro-industrial wastes and by-products, sugarcane bagasse (SB), in the form of pulpy fibrous material, is the main by-product of sugar industry after crushing the sugarcane to extract their juice. Because sugarcane from nature is the world's largest crop by production quantity with an annual output of more than 1.8 billion tons, SB is a widely available, cost effective, sustainable, and carbon neutral material. SB is commonly used as the primary fuel source for sugar mills and sometimes for pulping. The use of low-cost SB to adsorb cationic pollutants can realize the reuse of resources and is sustainable and affordable. Moreover, the SB after adsorption can be regenerated for continued use or burned to provide energy. Nevertheless, for large-scale applications, the main limitation of SB is their relatively low adsorption capacity due to their very limited anionic groups [7]. Furthermore, the complexity of SB, mainly composed of cellulose (45–55 wt%), hemicellulose (20–25 wt%), and lignin (18–24 wt%) (Fig. 1) [8], makes it difficult to be efficient chemical modified towards all three components. Various chemicals have been used to anionic modify the lignocellulosic biomass, including acids (citric acid, succinic anhydride, acrylonitrile, and

2-mercaptobutanedioic acid), bases (sodium hydroxide and sodium carbonate), oxidants (periodate, sodium hypochlorite, and potassium permanganate), and many other chemical compounds (thionyl chloride, epichlorohydrin, acrylonitrile, and hydroxylamine) [9, 10]. However, most of those modification reactions need long reaction time, high operational cost, and rigorous reaction conditions (high temperature and pressure). Additionally, extra efforts need to be paid to the second pollution caused by the modification reactions. Therefore, finding green modification ways to improve the adsorption performance of lignocellulosic biomass has a practical significance.

Ozone represents a promising modification reagent for increasing the anionic groups of materials because it's reactive, green, and cheap. Ozone is a strong oxidant with an extremely high oxidation potential of 2.07 eV. It has been used to react with organics and even inorganic substances under room temperature and pressure into products with carbonyl or carboxyl groups [11, 12]. Additionally, both the raw material and reaction product of ozone are usually oxygen, indicating the green nature of ozone modification. For lignocellulosic biomass, most studies focus on using ozone as a green oxidant to selective oxidize lignin, reducing its molecular weight and increasing its carboxyl and carbonyl groups, so as to improve its solubility for removal. However, a systematic study on using ozone to improve the adsorption performance of SB towards cationic organic pollutants is lacking in the literature.

In this study, we developed a simple and green method by using ozone to increase the adsorption performance of SB under room temperature and pressure (Fig. 1). The effects of ozone on the chemical compositions, total and surface anionic groups (carboxyl groups), and the absorption behavior
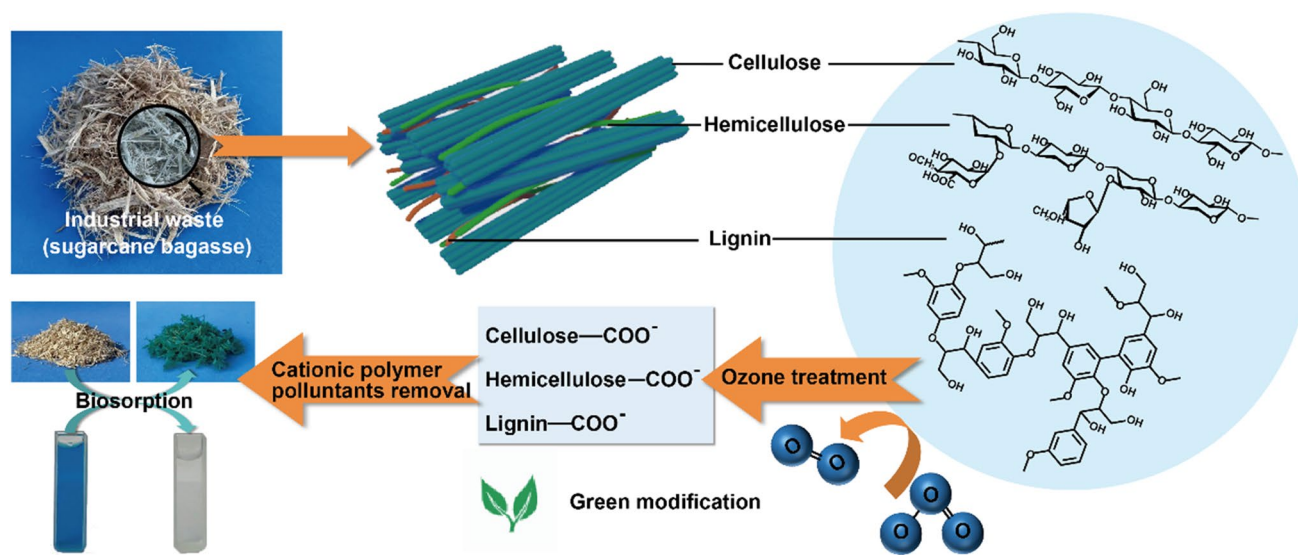

Fig. 1 Ozone modification of industrial waste (SB) to increase its anionic groups for cationic organic pollutants removal

of SB were investigated. Two types of cationic polymers were chosen in this study to investigate the adsorption abilities of the ozone-modified SB towards cationic pollutants with different charge densities, including poly (diallyl dimethyl ammonium chloride) (PDADMAC) with a high charge density and MB with a relatively low charge density. Ozone-modified SB showed enhanced adsorption capability towards cationic organic pollutants in the aqueous environment with low ozone consumption and high yield. Considering ozone as an efficient and green reactant, ozone-modified lignocellulosic biomass could be a promising adsorbent for removal of the cationic organic pollutants in the water bodies.

2 Materials and methods

2.1 Raw materials and chemicals

SB grown in South China was provided by a local pulp mill (Guangxi). It was washed three times with distilled water and dried at 60 °C before use. The dried SB was ground and crushed into small pieces by using a cutting mill (CM 200, Beijing Grinder Instrument Co., Ltd., China) equipped with a 4-mesh discharge screen. The crushed SB powder was vibrating separated by a circular vibrating screen (8411, Shangyu fifty-four Instrument Factory, China). The 20–40 mesh fraction of SB was collected and used in this experiment. grade H_2SO_4, NaOH, NaCl, and MB were used in this study.

2.2 Ozone treatment

Ten grams of SB was diluted to 40 wt% and its pH was adjusted to 2.0 by H_2SO_4 to improve the selectivity of subsequent ozone modification towards lignin. The obtained SB was transferred to a gas washing bottle. Ozone was fed from the bottom of stacked bagasse for 2.5 min, 5.0 min, 7.5 min, and 10.0 min, respectively. Ozone generator (GM 3, Primozone, Sweden) was used to generate ozone. The ozone concentration was detected by an ozone concentration detector (UV-2100, Usideal, China). The whole process was conducted under room temperature (23–25 °C) and pressure. Ozone consumption under different treatment time is listed in Table 1.

2.3 Characterization of SB and ozone-modified SB

2.3.1 Morphology analysis

Field emission scanning electron microscopy (FE-SEM, Merlin Compact, Zeiss, Germany) was used to investigate the morphology of SB at the ozone consumption of 0, 1.5 wt%, and 7.7 wt%.

Table 1 Ozone consumption at different treatment time

Sample	Ozone concentration (g/m^3)	Flow rate (L/min)	Time (min)	Ozone consumption (%)
0	0.0	0.0	0.0	0.0
1	154.7	1.5	2.5	1.5
2	156.5	1.5	5.0	3.0
3	152.2	1.5	7.5	4.4
4	166.8	1.5	10.0	7.7

2.3.2 Surface area and porosity analysis

The surface area of SB before and after ozone modification was measured by the surface area and porosity analyzer (ASAP 2460, Micromeritics Inc., USA). A total of 0.1 g of SB was degassed in vacuum at 120 °C for 24 h before testing.

2.3.3 FTIR analysis

Pellets of FTIR samples were prepared by mixing with 200 mg of spectroscopic grade KBr and 1-mg milled SB. IR spectra (4000–400 cm^{-1}) were recorded using a Nicolet 520P spectrometer (Nicolet Co., USA) with a resolution of 4 cm^{-1} and 64 scans per sample.

2.3.4 Composition analysis

The contents of cellulose, hemicellulose, and lignin in SB were examined according to NREL/TP-510–42,623 issued by the National Renewable Energy Laboratory (NREL). The experimental process is briefly described as follows: 0.3-g benzene-alcohol-extracted SB was treated by a double-stage H_2SO_4 hydrolysis (1st stage: 72 wt% acid, 30 °C, 1 h; 2nd stage: 4 wt% acid, 121 °C, 1 h). The obtained hydrolysate was then filtered by a G_4 filter. The hydrolyzed monosaccharides were performed using a high performance liquid chromatography (HPLC, Agilent 1260, Agilent Technologies, USA). The acid-soluble lignin was performed using a visible UV spectrophotometer (UV2600, Shimane Shimadzu Corporation, Japan). The G_4 filter was washed by distilled water until the filtrate was neutral and transferred into oven at 105 °C to a constant weight. Then transfer the filter to a muffle furnace for calcination at 575 ± 25 °C for 4 h to obtain the weight of the ash. The weight of the solid residue after deducting the weight of its ash is the weight of acid-insoluble lignin.

The selectivity coefficient of ozone towards lignin and carbohydrates (cellulose and hemicellulose) is calculated as follows:

$$Selectivity_{n-(n+1)} = \frac{Lignin_n - Lignin_{n+1}}{Carbohydr_n - Carbohydr_{n+1}} \qquad (1)$$

where $Selectivity_{n-(n+1)}$ represents the selectivity coefficient of ozone at the phase of $n-(n+1)$; $Lignin_n$ and $Carbohydr_n$ represent the lignin content (mg) and carbohydrates (mg) of Sample n, respectively; $Lignin_{n+1}$ and $Carbohydr_{n+1}$ represent the lignin content (mg) and carbohydrates (mg) of $Sample_{n+1}$, respectively.

2.3.5 Determination of the total carboxyl and carbonyl groups

Before the determination, the ozone-modified SB was milled into powder by the planetary ball mill (PQ-N2, Across International, USA). The total carboxyl content in SB was determined by conductometric titration. About 0.3 g of milled SB and 5 mL of 0.01 mol/L NaCl solution were dispersed into 50 mL of deionized water. The pH of the suspension was controlled at the range of 2.5–3.0 by 0.1 mol/L HCl solution. Before titration, the suspension was purged with an N_2 atmosphere at 25 °C for 30 min. The suspension was titrated by 0.1 mL standardized 0.1 mol/L NaOH with 60-s intervals until the electrical conductivity increased linearly; the electrical conductivity and the volume of NaOH were recorded for the calculation of the total carboxyl content [13].

The copper number was determined according to Tappi standard method (T 430 cm-09). The carbonyl content was linear correlated with the copper number and calculated by the following equation [14]:

$$CCOA = \frac{(Cu\# - 0.07)}{0.06} \qquad (2)$$

where $CCOA$ represents the total carbonyl content of SB (mmol/kg) and $Cu\#$ represents the copper number (%).

2.3.6 XPS analysis

Before XPS analysis, ozone-modified SB was extracted by dichloromethane to remove the extractives according to standard Tappi T 204 cm-07. XPS analysis was performed by X-ray photoelectron spectroscopy (Axis Ultra DLD, Kratos Analytical, UK) using a monochromated Al Kα source (5 mA, 15 kV). For the high-resolution spectra, the analytical area was 0.7 mm × 0.3 mm with a pass energy of 40 eV. All samples were tested three times. All spectra were fitted by XPS peak 4.1 using Lorentzian-Gaussian line shape (20% Lorentzian contribution) after Tougaard background correction.

The surface lignin ($\emptyset_{Lignin}$) of SB was calculated by the O/C ratios based on the XPS spectrum (Eq. 3) [15]. The calculated equation is as follows:

$$\infty_{Lignin} = \frac{O/C_{(sample)} - O/C_{(lignin-freeSB)}}{O/C_{(lignin)} - O/C_{(lignin-freeSB)}} \qquad (3)$$

where $O/C_{(sample)}$ is the O/C ratio of the SB sample after extraction, $O/C_{(lignin)}$ is the O/C value of lignin (0.33) [16]. The theoretical O/C value of cellulose is 0.83, the O/C value of the hemicellulose of SB is approximately 0.8 [17, 18], and the O/C value of delignified pulp is 0.8 [19]. Herein, the O/C $_{(lignin-free SB)}$ value of 0.8 was used in the equation to represent the lignin-free of SB.

2.4 Adsorption performance towards cationic organic polymers

2.4.1 Determination of MB adsorption

The sorption experiments were carried out by shaking 200 mL of MB solution with 1 g SB in an air bath shaker (200 rpm) at 30 °C. The pH of the initial solution was 6.0 adjusted by 0.1 mol/L HCl solution and 0.1 mol/L NaOH solution. The concentration of residual MB was examined using a UV–VIS spectrophotometer (UV-2600, Shimadzu, Japan) at the wavelength of 665 nm. A standard calibration curve was built by different concentrations of MB solution (0, 1, 2, 3, 4, 5 mg/L) with a linear correlation coefficient of 0.999. The adsorbed MB was calculated as the following equation:

$$Q = \frac{(C_0 - C)V}{M} \qquad (4)$$

where Q represents the content of adsorbed MB (mg/g); V represents the volume of the solution (L); C_0 represents the initial concentration of MB (mg/L); C represents the concentration of MB (mg/L), and M represents the mass of the sample (mg).

For kinetic studies, the initial concentration of MB was 100 mg/L MB. The concentration of residual MB was examined at different time intervals (0 ~ 100 min). For adsorption isotherm studies, different initial concentrations (0 ~ 100 mg/L) of MB were used. The equilibrium concentration of the residual MB was examined after 24 h of adsorption. The adsorption equilibrium was reached after 24 h of adsorption, and the concentration of residual MB was examined. The effects of pH (3 ~ 9) and NaCl (0.01 M and 0.6 M) concentrations on the adsorption capacity were studied when the initial concentration of MB was 100 mg/L. Each experiment was repeated at least three times, and the data shown was averaged.

Table 2 Mathematical expressions of the three kinetic models

Kinetic model	Equation	Integrated form
Irreversible first-order	$dq/dt = k_I(q_e - q)$	$log(q_e - q) = log q_e - (k_I/2.203)t$
Reversible first-order	$dc/dt = k_1 C - k_{-1} X$	$-ln((C - C_e)/(C_0 - C_e)) = kt$
Pseudo-second-order	$dq/dt = k_{II}(Q_e - Q)^2$	$t/Q = 1/(k_{II} q_e^2) + t/q_e$
Nonlinear pseudo-second-order	$dq/dt = k_{II}(Q_e - Q)^2$	$Q = k_{II} q_e^2 t/(1 + q_e t)$

Table 3 Mathematical equations of three adsorption isotherm models

Adsorption isotherm model	Equation
Langmuir	$Q_e = (Q^0 K_L C_e)/(1 + K_L C_e)$
Freundlich	$Q_e = K_F C_e^{1/n}$
Redlich–Peterson	$Q_e = (A_R C_e)/(1 + K_R C_e^{\beta})$

Four kinetic models, namely irreversible first-order, reversible first-order, pseudo-second-order models, and non-linear pseudo-second-order (Table 2), were adopted to reveal the mechanism of the ozone-modified SB participating in the MB adsorption process.

Where t is the adsorption time (min), q is the amount of MB adsorbed per unit of SB at time t (mg/g), k_I is the rate constant for first-order kinetic model (min^{-1}), Q is amount of MB adsorbed per unit of SB at time t (mg/g), Q_e is the experimental amount of MB adsorbed per unit of SB (mg/g), q_e is the calculated amount of dye molecules adsorbed per unit of SB (mg/g), k_1 is the forward reaction rate constant, k_{-1} is the reverse reaction rate constant, k is the equilibrium rate constant for e reversible kinetic model (equal to the ratio of k_1 to k_{-1}), c is the initial concentration of MB at time t (mg/L), X is the MB in the solid phase, C_0 is the initial concentration of MB (mg/L), C_e is the equilibrium concentration of MB (mg/L), C is the concentration of MB (mg/L) at time t, k_{II} is the rate constant of pseudo-second-order kinetic model (g mg^{-1} min^{-1}).

For adsorption isotherm studies, three widely used equilibrium models, namely Langmuir, Freundlich, and Redlich–Peterson (Table 3), were adopted.

Where Q^0 is Langmuir monolayer adsorption capacity (mg/g), K_L is Langmuir isotherm constant (L/mg), K_F is Freundlich isotherm constant ((mg/g) (L/mg)$^{(1-n/n)}$), n is Freundlich exponent related to adsorption intensity, A_R is Redlich–Peterson isotherm constant (L/mg)$^{\beta}$, K_R is Redlich–Peterson isotherm constant (L/g), β is Redlich–Peterson exponent.

The thermodynamic parameters were calculated by the following equations:

$$K_a = \left(\frac{C_0 - C_e}{C_e}\right) \times \frac{V}{M} \quad (5)$$

$$\Delta G^o = -RT ln K_a \quad (6)$$

$$\Delta G^o = \Delta H^o - T\Delta S^o \quad (7)$$

where K_a is the dimensionless separation factor (L/mol), C_0 and C_e are the initial and equilibrium MB concentrations (mg L^{-1}), V is the volume of MB solution (mL), M is the mass of the sample (mg), R is the universal gas constant (8.314 J/(mol·K)), T is the temperature (K), ΔG° is the Gibb's free energy change, ΔH° is the enthalpy change, ΔS° is the entropy change.

2.4.2 Determination of adsorption of PDADMAC

To investigate the effects of ozone modification on improving the adsorption of SB to highly charged cationic pollutants, a highly charged polymer (PDMAC) and a particle charge detector (PCD-03 pH, Mütek™, Germany) were used. A total of 0.1-g milled sample was dispersed in 10 mL deionized water and titrated by 0.001 N standardized PDADMAC solution. The adsorption capability was calculated as the following equation:

$$p = \frac{c * V}{m} \quad (8)$$

where p represents the adsorption capability of SB towards PDADMAC (mmol/kg); V represents the volume of PDADMAC used (mL); c represents the concentration of PDADMAC (mmol/mL), and m represents the weight mass of the sample (kg).

3 Results and discussion

3.1 Effects of ozone modification on the morphology of SB

Ozone modification we developed was green and sustainable without requiring harsh reaction conditions (high temperature and pressure), toxic chemicals, and high chemical load. Besides, the original shape and size of SB were also maintained, thereby ensuring that the modified SB could be easily recycled from water bodies. The detailed ozone modification process of SB is illustrated in Fig. 2a. Under room temperature and pressure, a continuous flow of ozone with a concentration of 150 ~ 170 g/m^3 produced by the
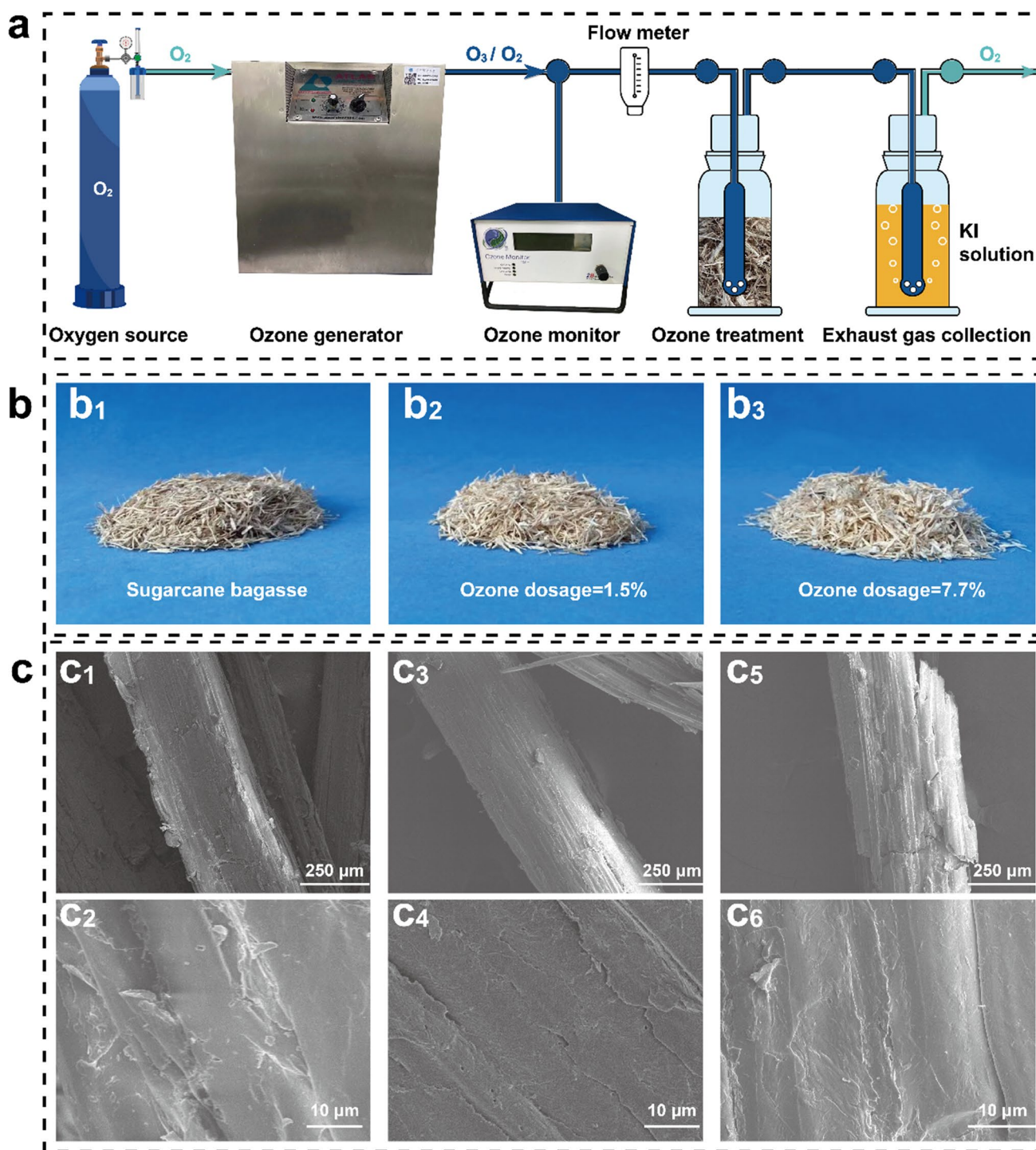
Fig. 2 **a** Schematic image of ozone modification process. **b** Photos showing original SB (b_1) and ozone-modified SB with an ozone consumption of 1.5 wt% (b_2) and 7.7 wt% (b_3). **c** SEM images of original SB (c_1 and c_2) and ozone-modified SB with an ozone consumption of 1.5 wt% (c_3 and c_4) and 7.7 wt% (c_5 and c_6)

ozone generator entered the gas-washing bottle containing 10-g SB at the flow rate of ~ 1.5 L/min. The total ozone consumption was between 1.5 ~ 7.7% of the weight of SB. After the ozone treatment, there was no significant change

in the morphology of SB at the macro scale, but the color became lighter (Fig. 2b1–b3), which could be due to the oxidative degradation of lignin by ozone. Lignin is rich in the chromophore groups and is the main color source of most

lignocellulosic biomass. Ozone could effectively cleave the chromophore groups of lignin and further oxidize them to carboxyl or aldehyde groups, resulting in a decrease in the polymerization degree (DP) and an increase in the solubility of the lignin, which ultimately lead to the decreased lignin content and chromophore groups in SB [20].

To investigate the effects of ozone on the microstructure of SB, the SB before and after ozone modification was characterized by SEM. As can be seen from Fig. 2c1, c3, and c5, similar to the macrostructure, the microstructure of SB was also maintained. While the chemical compositions of the SB surface had undergone major changes (Fig. 2c2, c4, and c6), which played an important role in the adsorption rate. As shown in Fig. 2c2, the surface of the original SB was covered by melted substances, which could be composed of lignin [19]. When the ozone consumption was 1.5 wt%, the surface of ozone-modified SB (Fig. 2c4) had significantly fewer melted substances, but the melted substances could be clearly observed again when the ozone consumption attained 7.7 wt% (Fig. 2c6). This revealed that the partially dissolved lignin modified by ozone could re-deposit onto the surface of SB due to the increase in pH during the washing process [21].

To investigate the effects of ozone on SB morphology, the porosity and surface area of natural and ozone-modified SB were also characterized. BET method was used for surface area evaluation, and BJH desorption method was used for pore diameter and volume characterization. As shown in Table 4, the average pore diameter, total pore volume, and the average of the SB were found to be 311.23 Å, 0.0029 cm^3/g, and 0.37 m^2/g. After ozone modification, the surface area and pore volume of the SB increased significantly, while the average pore diameter decreased (especially for sample 1). This could be due to a large number of small pores which were generated during the rapid degradation of lignin by ozone. With the increase of ozone consumption, lignin is further degraded, resulting in an increase in average diameter and pore volume and in a decrease in surface area. In summary, ozone modification can basically maintain the SB morphology at the macro- and micro-scales, while significantly increasing the specific surface area and porosity of SB, especially at low ozone dosage (~ 1.5 wt%), which is beneficial to improve its adsorption performance.

Table 4 Comparison of the porosity and surface area of SB before and after ozone modification

Sample	BET surfacearea (m^2/g)	Total porevolume (cm^3/g)	Average porediameter (Å)
0	0.37	0.0029	311.23
1	0.88	0.0040	207.71
4	0.63	0.0049	281.20

3.2 Effects of ozone on the compositions and functional groups of SB

To improve the adsorption capability of SB towards cationic organic pollutants, ozone modification was used to increase its carboxyl content. Figure 3a1–a3 showed the ozone modification towards the three main components (cellulose, hemicellulose, and lignin) in SB. For lignin, ozone has high reactivity and selectivity to its aromatic and olefinic structures. Ozone first reacts with the double bonds in lignin through 1,3-dipolar addition to form primary ozonide, which is then hydrolyzed into muconic acid derivatives (containing carbonyl and carboxyl groups) and hydrogen peroxide (Fig. 3a1) [20]. Moreover, with the further increase in ozone consumption, the aromatic structures and double bonds of the side chains of lignin would be cleaved to small molecules of high hydrophilic fatty acids, causing partial removal of lignin from the SB [11]. For carbohydrates (cellulose and hemicellulose), ozone can directly attack the glycosidic bonds to form hydrogen trioxide, which was then cleaved to form lactone and oxygen. Finally, carbohydrates were hydrolyzed to form a carboxyl-containing structure (Fig. 3a2 and a3) [20].

To further investigate the effects of ozone modification towards the compositions and functional groups of SB, Fourier transform infrared spectroscopy (FTIR) was used (Fig. 3b). Regarding the change of functional groups, after ozone modification, the adsorption bands at 1637 cm^{-1} and 1735 cm^{-1} assigned to the C=O stretching of carboxylate (-COO$^-$) and free carboxyl groups (-COOH) were strengthened, which confirmed the effects of ozone on increasing the carboxyl groups of SB [21]. Regarding the change of compositions, it can be seen that the absorption bands at 1425 cm^{-1}, 1514 cm^{-1}, and 1604 cm^{-1} assigned to the aromatic skeleton vibrations in lignin structure were weakened after ozone modification. Meanwhile, the absorption band at 897 cm^{-1} assigned to the C–O–C stretching vibration of glycosidic bond of carbohydrates (cellulose and hemicellulose) was strengthened. This indicated that ozone exhibited high selectivity to aromatic structures of lignin than the glycosidic bonds of carbohydrates. Besides, due to the decrease content of the lignin, the SB exhibited more hydroxyl groups (3406 cm^{-1} OH stretching vibration strengthened) after ozone modification [22]. Overall, ozone can react with all the three main components in SB to generate carboxyl-containing derivatives, indicating the high feasibility of using ozone to improve the adsorption capability of SB towards cationic organic pollutants.

3.3 Composition analysis of SB before and after ozone modification

Composition analysis could directly show the effects of ozone modification on the cellulose, hemicellulose, and
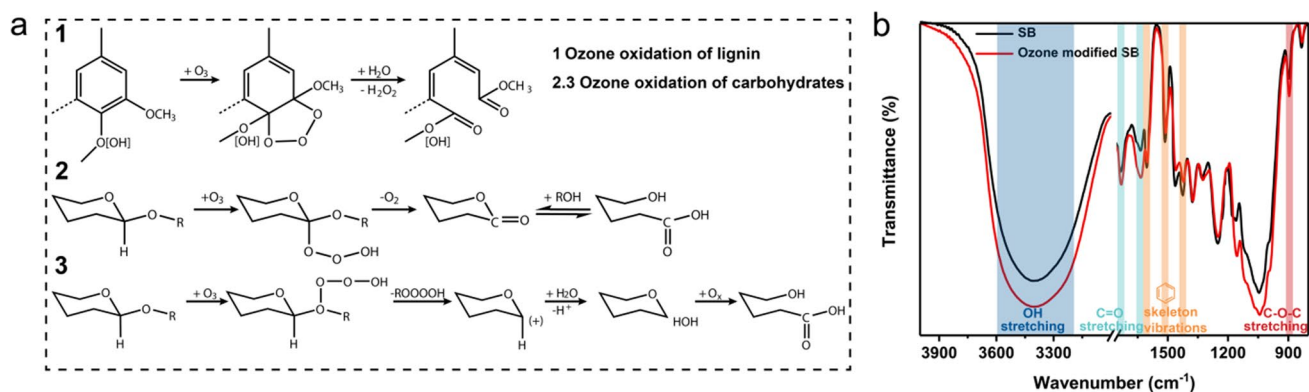
Fig. 3 **a** Ozone modification reaction towards the three main components (lignin (1), cellulose and hemicellulose (2 and 3)) of SB. **b** FTIR spectrum of SB before (black line) and after ozone modification (sample 1, red line)

lignin of SB. The changes of the three main chemical components of SB with the ozone consumption are illustrated in Fig. 4a. Since ozone is an effective reactant, the contents of all three components decreased with the increase of ozone consumption. When the ozone consumption was only 1.5 wt% (sample 1), the yield of ozone-modified SB was as high as 95.9 wt%, the total lignin decreased about 21.9 wt%, whereas the cellulose and hemicellulose decreased only about 1.7 wt% and 0.19 wt%, respectively. As the ozone consumption reached to 7.7 wt% (sample 4), a high yield (88.4%) was still obtained, the decrease of total lignin slowed down (33% decrease) but the decrease of cellulose and hemicellulose increased (3.8% for cellulose and 6.1% for hemicellulose).

Ozone showed high selectivity to lignin, especially when the lignin content of SB was high (Fig. 4b). This could be because ozone has higher reactivity towards aromatic and side-chain-olefin of the lignin structure than the glycosidic bonds of carbohydrates [20]. The selectivity of ozone towards lignin decreased quickly as the decrease of total lignin content. Meanwhile, the selectivity of ozone towards cellulose and hemicellulose increased quickly (Fig. 4b). This indicated that the oxidation tended to occur on the surface of SB rather than inside the SB due to its compact structure, despite the presence of large amounts of pores. Once the lignin on the surface was reduced to some extent, the oxidation of the cellulose and hemicellulose exposed from the covered lignin could increase, thus causing the rapid weight loss of carbohydrates (cellulose and hemicellulose). In addition, the hydroxyl contents of cellulose, hemicellulose, and lignin were about 18.52 mmol/g, 14.43 mmol/g, and 5.29 mmol/g, respectively [23]. The high weight loss of lignin and low weight loss of cellulose and hemicellulose indicated that the relative content of the hydroxyl group in ozone-modified SB increased, which was beneficial to increase the hydrophilic properties of SB and therefore improve the adsorption rate of SB.

Interestingly, compared to the original SB, only acid-insoluble lignin in total lignin decreased, while acid-soluble lignin increased during the ozone modification. The increased acid-soluble lignin value remained constant after the ozone consumption reached 1.5 wt% (sample 1). This could be attributed to the decrease of DP of acid-insoluble lignin and the increase of carboxyl groups, which transformed acid-insoluble lignin into acid-soluble lignin [24]. Acid-soluble lignin would be further oxidized to small molecule acids or even to carbon dioxide and water [20]. The constant value of acid-soluble lignin could be due to the balance between the oxidation of acid-insoluble lignin and acid-insoluble lignin. Additionally, the increase of acid-soluble lignin also meant the increase of carboxyl groups of lignin in SB.

It could be concluded from above that ozone showed high selectivity towards lignin and increase the functional groups of SB with low ozone consumption. The increase of functional groups in SB, including hydroxyl and carboxyl groups, could be benefited for its adsorption abilities in terms of adsorption capability and adsorption rate. To further find out the effects of ozone on the functional groups of ozone-modified SB, the total and surface functional groups (carboxyl and carbonyl groups) were tested.

3.4 Characterization of functional groups in the ozone-modified SB

The contents of carbonyl and carboxyl groups are important parameters reflecting the reaction behavior of ozone to SB and the potential of ozone modification for anionic groups increases. The change of total carbonyl and carboxyl groups with the ozone consumption was illustrated in Fig. 4c and d. After ozone modification, both the contents of carboxyl and carbonyl groups increased. The carboxyl groups increased first and then tended to gentle as the increase of ozone consumption. Meanwhile, the carbonyl groups increased first

Fig. 4 **a** Effects of different ozone consumption on the chemical compositions of ozone modified SB. **b** Selectivity coefficient change with ozone consumption. Effects of ozone consumption on the **c** total carboxyl and **d** carbonyl groups of the ozone modified SB. **e** and **f** The XPS spectra of extractives-free ozone modified SB with different ozone consumption.
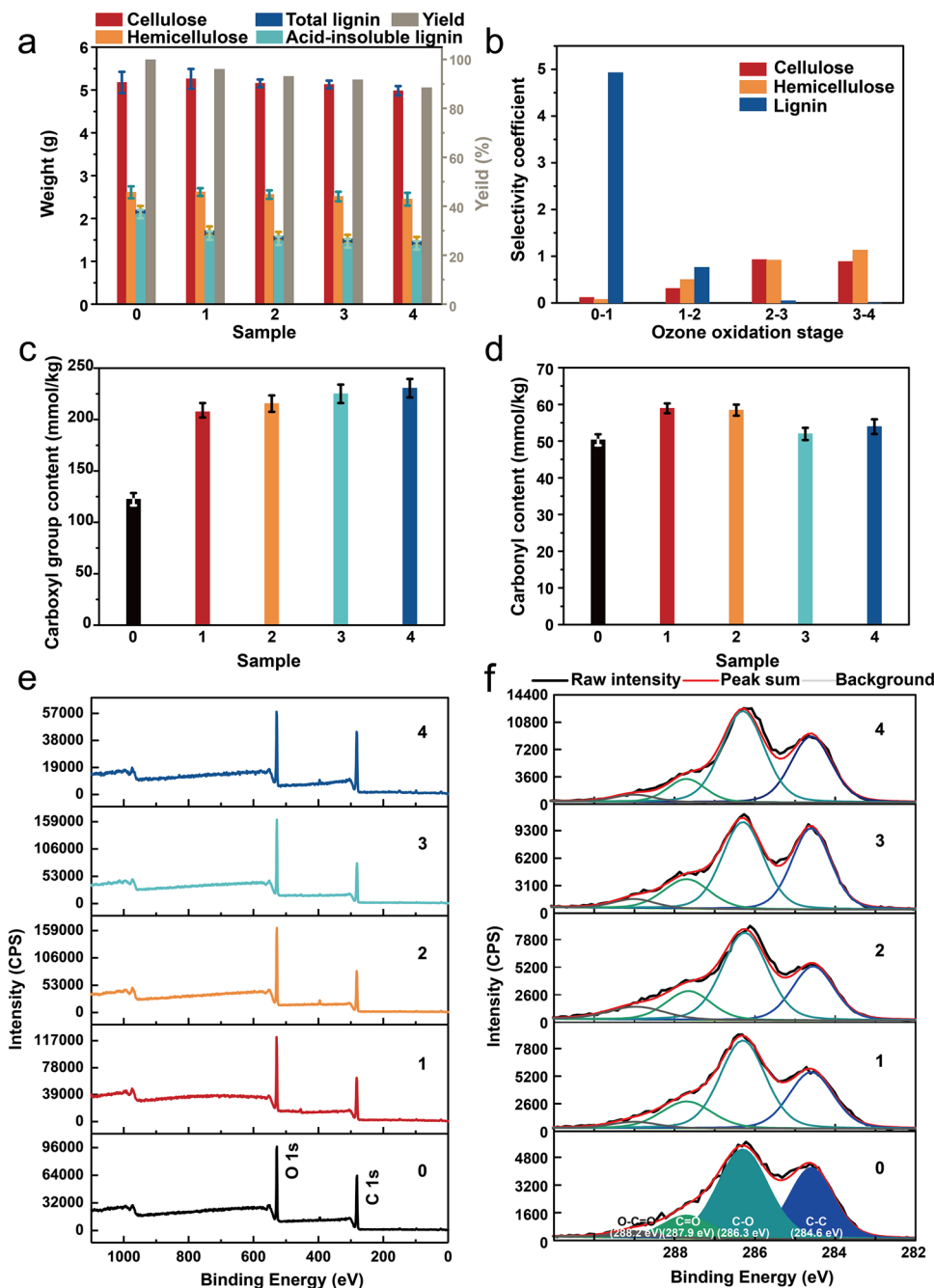
and then slightly decreased with the increase of ozone consumption. This change could be closely related to the composition change during the ozone modification. Before ozone consumption attained at 3.01 wt% (sample 1 and sample 2), the increase of carboxyl and carbonyl groups was accompanied by the rapid decrease of lignin content (Fig. 4a). A certain amount of carbonyl and carboxyl groups was formed through the reaction of ozone with the olefin and aromatic structures of lignin [25].

When ozone consumption was beyond 3.01 wt% (sample 3 and sample 4), the composition change was dominated by

the degradation of carbohydrates, thus causing the changes of functional groups (Fig. 4a). This process can be divided into three steps [26]: the formation of carbonyl groups, followed by oxidation to carboxyl groups, and decarboxylation [27]. The reason for the steady state of carboxyl content could be that the rate of oxidation of the carbonyl groups to carboxyl groups was approximately equal to that of decarboxylation [27]. Importantly, the total carboxyl and carbonyl groups were increased about 84.1% and 16.1% (sample 1) with an ozone consumption of only 1.5 wt%. Overall, ozone modification effectively increased the total content

of carboxyl groups of SB under the conditions of high yield and low ozone consumption.

The surface chemical properties (including compositions and functional groups) have significant effects on its physicochemical properties and are the important factors for the adsorption rate from dilute aqueous solutions [28–30]. XPS analysis was used to determine the carboxyl and carbonyl contents on the surface of extractive-free SB (Fig. 4e and f). The XPS analysis of extractive-free SB revealed four C peaks at 284.6, 286.3, 287.9, and 288.2 eV (Fig. 4f), originating from C1 (C–C), C2 (C-O), C3 (O-C-O and/or C=O), and C4 (O-C=O), respectively [31]. Carbohydrates exhibited two peaks in the XPS spectrum, C2 (alcohols and ethers), and C3 (ketones and aldehydes). The peak C1 (aliphatic carbon) only originated from the lignin of extractives-free SB, because the extractives have been removed by extraction and C–C bonds do not exist in the carbohydrates.

The relative intensities of four peaks, O/C ratios, and the calculated surface lignin contents of the ozone-modified SB with different ozone consumption are shown in Table 5. Unlike the decrease of the total lignin content, the content of surface lignin first decreased and then increased with the increase of the ozone consumption. According to the results of composition analysis, there were two stages in the ozone modification process, namely rapid weight loss of lignin and rapid weight loss of carbohydrates. Similar stages could also exist for the surface composition of SB. Since $\varnothing_{Lignin}$ is the relative content of lignin, the decrease of $\varnothing_{Lignin}$ could be mainly due to the partial dissolution of the lignin during the first stage. Subsequently, the increase of $\varnothing_{Lignin}$ could be due to the rapid degradation of carbohydrates during the second stage and the re-deposition of dissolved lignin, which was consistent with the SEM results.

The change of carboxyl groups on the surface of SB can be indicated by the relative intensity of C4 (carboxylic acid and ester). In Table 5, both the content of carbonyl and carboxyl groups first increased and then decreased with the increase of ozone consumption. This result could be closely related to the carboxylation reaction of ozone and the surface composition change of SB. The carboxylation reaction

of ozone towards all three components could significantly increase the carboxyl groups of SB and decrease the content of surface lignin. The subsequent decrease could be due to the re-deposition of dissolved lignin with a certain carboxyl content. The carboxyl groups on the SB surface increased dramatically during the ozone modification with a maximum increase of 257% at the ozone consumption of 3.0 wt%. When the ozone consumption reached 7.7 wt%, the carboxyl groups still increased about 132%. Overall, after ozone treatment, the surface of SB contained increased anionic groups (carboxyl groups) and a decreased content of hydrophobic lignin, which could be beneficial to its adsorption performance.

3.5 Adsorption of cationic organic polymers by SB and ozone-modified SB

To investigate the adsorption abilities of the ozone-modified SB towards cationic organic pollutants, batch adsorption experiments were carried out by using 1 g of ozone-modified SB in 200 mL of 100 mg L^{-1} MB solution with a pH of 6 at 30 °C. As illustrated in Fig. 5a, the adsorption of MB can be divided into three stages, namely the rapid adsorption period, slow adsorption period, and the equilibrium adsorption period [32, 33]. The above three stages were controlled by film diffusion, intraparticle diffusion, and the physisorption and chemisorption, respectively. During the adsorption process, MB molecules first diffused from the solution to the external surface of the adsorbent (film diffusion), then migrated to the interior surface (intraparticle diffusion), and finally adsorbed on the surface sites of SB (physisorption or chemisorption) [32, 34]. By increasing the hydrophilic groups (hydroxyl and carboxyl groups) and cation binding sites (carboxyl groups) of SB, the ozone-modified SB exhibited a higher adsorption rate, especially at the early stage of adsorption, as well as a higher adsorption capacity than that of the original SB (Fig. 5a). Furthermore, according to the results of adsorption equilibrium experiments (listed in Table 6), among all the ozone-modified SB, sample 1 exhibited the

Table 5 XPS analysis of the extractives-free ozone-modified SB with different ozone consumption

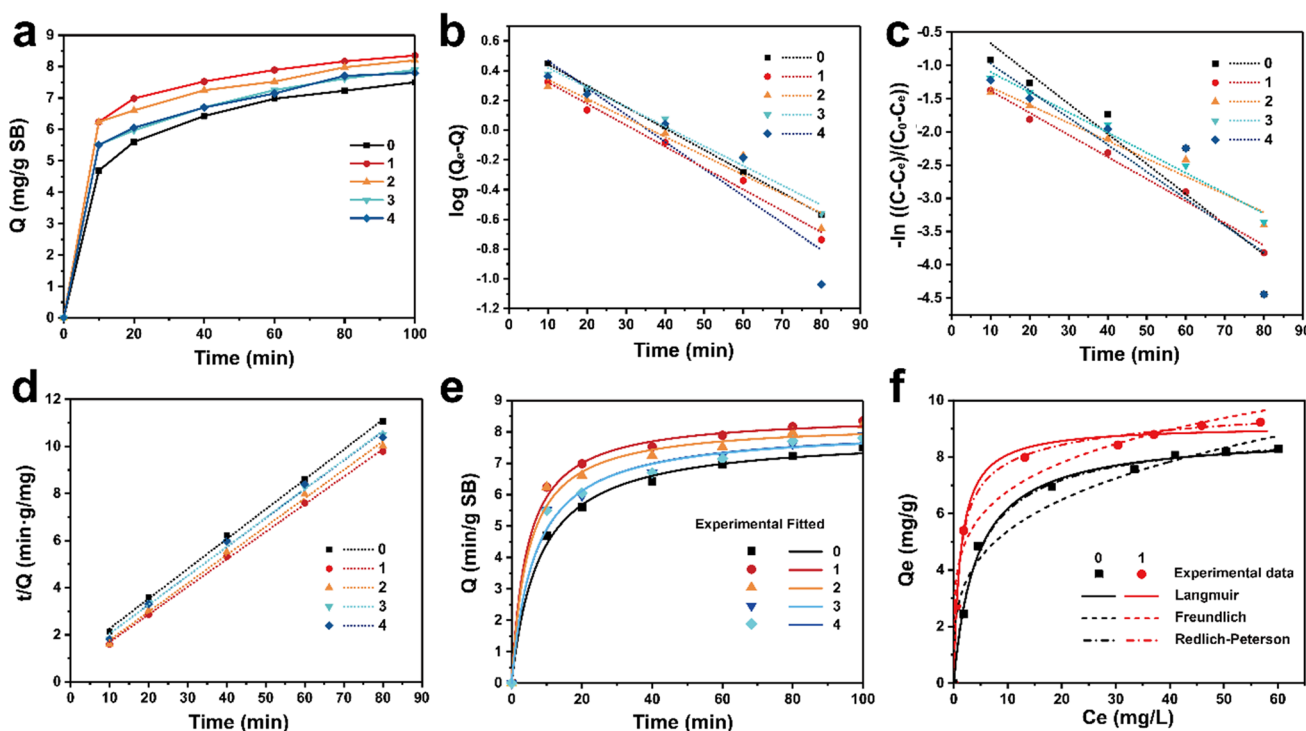| Sample	Ozone consume charge (%)	O/C	Binding energy				$\varnothing_{Lignin}$ (%)
			C1 (%)	C2 (%)	C3 (%)	C4 (%)	
			C–C	C-O	C=O	O-C=O	
			284.6 eV	286.3 eV	287.9 eV	288.2 eV	
0	0.0	0.50	35.6	49.6	12.0	2.8	65
1	1.5	0.59	30.2	51.2	14.2	4.3	48
2	3.0	0.60	26.4	48.8	14.8	10.0	47
3	4.4	0.56	36.6	46.1	11.1	6.3	55
4	7.7	0.52	34.4	47.1	12.1	6.5	61

Fig. 5 Adsorption of MB by the ozone-modified SB. **a** The adsorption curves for MB onto the ozone-modified SB (SB concentration = 5 g/L, initial solution pH = 6, temperature = 30 °C), **b** linear irreversible first-order, **c** reversible first-order, **d** pseudo-second-order, and **e** nonlinear pseudo-second-order kinetic plots of MB adsorption onto SB and ozone-modified SB with different ozone consumption. **f** Langmuir, Freundlich and Redlich–Peterson isotherms fitting curves for MB adsorption by SB (sample 0) and ozone-modified SB (sample 1)

Table 6 Kinetic rate constants related to the biosorption of MB onto SB and ozone-modified SB

	Sample				
	0	1	2	3	4
Irreversible first-order					
k_I (min^{-1})	0.033	0.042	0.033	0.029	0.030
Calculated qe (mg/g)	3.857	4.452	2.923	2.924	3.560
R^2	0.998	0.841	0.983	0.927	0.977
Reversible first-order					
k	0.045	0.033	0.027	0.030	0.041
R^2	0.827	0.983	0.942	0.977	0.775
Pseudo-second-order					
k_{II} (g mg^{-1} min^{-1})	0.016	0.027	0.026	0.019	0.019
Calculated q_e (mg/g)	7.886	8.540	8.295	8.117	8.143
R^2	0.999	0.999	0.997	0.996	0.994
Nonlinear pseudo-second-order					
k_{II} (g mg^{-1} min^{-1})	0.017	0.030	0.033	0.023	0.024
Calculated q_e (mg/g)	7.870	8.481	8.177	7.994	7.944
R^2	0.997	0.998	0.992	0.990	0.991
Experimental q_e (mg/g)	8.295	9.237	9.063	8.725	8.613

Where R^2 is the squared regression correlation coefficient

largest equilibrium adsorption capability of 9.237 mg/g SB, 11.3% higher than the original SB (8.295 mg/g SB), and the largest adsorption rate of 0.624 mg g^{-1} min^{-1} after 10 min of contact with MB, 33.3% higher than original SB (0.416 mg g^{-1} min^{-1}). As the ozone consumption charge further increased, both the maximum adsorption rate and adsorption capacity of SB slightly decreased.

To reveal the mechanism of the ozone-modified SB participating in the MB adsorption process, three kinetic models were adopted, namely irreversible first-order, reversible first-order, and pseudo-second-order models (Table 2) [35, 36]. The irreversible first-order model is derived as the assumption that once adsorbed, the particle cannot diffuse along or desorb from the surface. The reversible first-order model is derived under the assumption that the adsorption and desorption rate constants are equal to the equilibrium reaction rate constant [37, 38]. As for the pseudo-second-order model, which is contrary to the previous models, it assumes the "chemisorption" behavior over the whole biosorption process [35].

From Fig. 5b–d and Table 6, compared to the other two models, pseudo-second-order model was the best fitted model for both original and ozone-modified SB with a R^2 higher than 0.990. This indicated that the adsorption of

MB by SB was more like the chemisorption-based process involving ions exchange between MB^+ ions and functional groups (mainly -OH and -COOH) of SB [39–41]. In addition, since the nonlinear regression method was believed to be more appropriate for determining the rate kinetic parameters [42, 43], nonlinear pseudo-second-order kinetic model was also adopted in this study (Table 2). As shown in Fig. 5e, the nonlinear pseudo-second-order kinetic plots correlated well with the experimental data ($R^2 > 0.990$). The related adsorption parameters (k_{II} and q_e, Table 6) were very close to that of linear pseudo-second-order model (k_{II} and q_e) and the experimental data (q_e), which further confirmed that the pseudo-second-order model could be suitable for investigating the adsorption mechanisms of SB towards MB. Therefore, the change of adsorption rate and equilibrium adsorption capacity could be closely related to the change of functional groups during the ozone modification.

With the increase of ozone consumption, the change of adsorption rates of SB with different ozone consumption correlated well with the changes of hydroxyl and carboxyl groups on its surface, which can be indicated by O/C ratios and C4 relative intensity in Table 5. Since the maximum adsorption rate was reached at the early stage, the increased hydrophilic hydroxyl and carboxyl groups on the surface could enhance the hydrophilicity, thereby promoting the permeation of water as well as the MB molecules through the film, and finally increasing the adsorption rate [44]. The increase of the carboxyl groups could lead to the increase of chemisorption sites for cationic organic pollutants, which in turn increased the adsorption capacity of ozone-modified SB. Moreover, the reason for the decrease of equilibrium adsorption capability of SB with high ozone consumption could be that the redeposited lignin as one of the important sources of adsorption sites (carboxyl groups) for MB could redissolve into the solution during the adsorption process, thus reducing its adsorption capability.

To optimize the design of adsorption system, three widely used nonlinear equations, namely Langmuir, Freundlich, and Redlich–Peterson (Table 3), were adopted to simulate the experimental equilibrium adsorption capabilities of SB (sample 0) and ozone-modified SB with the highest adsorption capability (sample 1) [45–47]. Figure 5f showed the fitting adsorption isotherms of the above equations, and the corresponding fitting constants were listed in Table 7. As shown, the Langmuir and Redlich–Peterson models of both SB and ozone-modified SB had higher R^2 (> 0.995) and were better fitting than the Freundlich model (~0.972). In addition, the β in the Redlich–Peterson model of both SB (0.98) and ozone-modified SB (0.95) was approximately 1, which indicated that the isotherm was closer to the Langmuir isotherm than the Freundlich isotherm. Therefore, the high fitting between Langmuir and Redlich–Peterson models

Table 7 Adsorption isotherm constants related to the biosorption of MB onto SB (sample 0) and ozone-modified SB (sample 1)

	Sample	
	0	1
Langmuir		
Q^0 (mg/g)	8.39	9.31
K_L (L/mg)	0.28	0.72
R^2	0.995	0.995
Freundlich		
K_F [(mg/g) (L/mg)$^{(1-n/n)}$]	2.88	4.27
n	3.68	4.97
R^2	0.973	0.972
Redlich–Peterson		
A_R (L/mg)$^\beta$	2.20	8.97
K_R (L/g)	0.28	1.19
β	0.98	0.95
R^2	0.996	0.999

and experimental results confirmed the monolayer coverage process of MB onto SB and ozone-modified SB [37]. On the other hand, the Langmuir saturation capacity Q^0 and Freundlich adsorption intensity n of SB increased after ozone modification, which confirmed that the increase of adsorption capacity was closely related to the increase of chemical binding sites.

Table 8 compares the Q^0 and n of our SB and ozone-modified SB with other sorbents mentioned in the literature to reveal the potential of using ozone-modified SB to remove MB from aqueous solutions. As seen that ozone-modified SB could be an efficient sorbent for MB removal when compared to some biosorbents, inorganic sorbents, or bio-derived active carbons [35, 37, 39–52]. Although the adsorption capacity of ozone-modified SB for MB still has great room for improvement compared with commercial adsorbents, ozone-modified agricultural waste (SB) is low and sustainable. The amount of ozone used for modification was 15 kg/ton SB (1.5 wt% ozone consumption) with a cost of only US $72/ton. In addition, based on the above results and its potential mechanisms, ozone modification could be an effective and commercially feasible method to further improve some lignocellulosic biomass with high adsorption capacity (for example, rice husk, Table 8).

When removing cationic pollutants from the water bodies, it is important to consider the effect of NaCl concentration on the adsorption performance of adsorbent because the seawater (~0.6 M NaCl solution) and wastewater could contain a high concentration of salt. Figure 6a shows the effect of the NaCl concentration on the equilibrium adsorption capability of the SB and ozone-modified SB (sample 1) towards MB. Both the equilibrium adsorption capability of SB and ozone-modified SB decreased as the NaCl concentration increased,

Table 8 Comparison of adsorption isotherm constants of Langmuir and Freundlich models between SB (sample 0) and ozone-modified SB (sample 1) with other sorbents mentioned in the literature

Sample	Langmuir constants			Freundlich constants			References
	Q^0	K_L	R^2	K_F	n	R^2	
SB	8.39	0.28	0.995	2.88	3.68	0.973	This study
Ozone-modified SB	9.31	0.72	0.995	4.27	4.97	0.972	This study
Raw *Posidonia oceanica* fibers	5.56	0.22	0.997	1.20	1.98	0.985	[37]
Neem leaf powder	3.76	0.18	0.960	2.42	0.56	0.990	[48]
Fly ash	5.57	0.54	0.996	4.38	18.2	0.882	[49]
Red mud	2.45	0.28	0.930	-	0.58	0.970	[50]
Coir pith activated carbon	5.78	0.93	0.973	0.85	0.71	0.867	[51]
Rice husk	40.6	0.14	0.985	8.63	2.76	0.968	[52]

which could be due to the competitive effects between the Na^+ and MB^+ ions on the binding sites available for adsorption. In addition, after ozone modification, the increased available sorption sites made the ozone-modified SB more resistant to salt water than the original SB. The adsorption capability of original SB in 0.6 M NaCl solution decreased 29.0% than in 0.01 M NaCl, while that of ozone-modified SB only decreased 17.7%.

In addition to salt concentration, pH is also an important factor affecting dye adsorption, because it affects the chemical binding sites of SB and the ionization process of MB molecules. Figure 6b shows the equilibrium adsorption capability of SB ad ozone-modified SB at the pH of 3, 6, and 9. As shown, the equilibrium adsorption capacity of SB and ozone-modified SB was basically the same at

pH 6 and 9, but it decreased at pH 3 (16.6% decrease for SB, 13.9% decrease for ozone-modified SB). This could be attributed to the competitive effects between the H^+ and MB^+ ions on the binding sites available for adsorption. Take the carboxyl group as an example, at low pH, the carboxylate groups ($-COO^-$) tended to be protonated to form carboxyl groups ($-COOH$). When the pH of the electrolyte increased from 3 to 6 and 9, the carboxyl groups (-COOH) tended to be deprotonated to form the available binding sites (-COO$^-$), which was favorable to improve adsorption capacity towards MB^+ ions [54]. Similar phenomenon is also found in the ionization process of MB molecules. Therefore, both SB and ozone-modified SB showed a pH-responsive adsorption behavior, which was consistent with other lignocellulosic biosorbents [37].

Fig. 6 Comparison of adsorption capacities of SB and ozone-modified SB under different conditions. **a**, **b**, and **c** Effects of NaCl concentration (0.01 M and 0.6 M), pH (3, 6, and 9), and temperature (293 K, 303 K, and 313 K) on the adsorption capability of SB (sample 0) and ozone-modified SB (sample 1). **d** comparison of adsorption curves of SB and ozone-modified SB for MB and Congo red (anionic dyes)
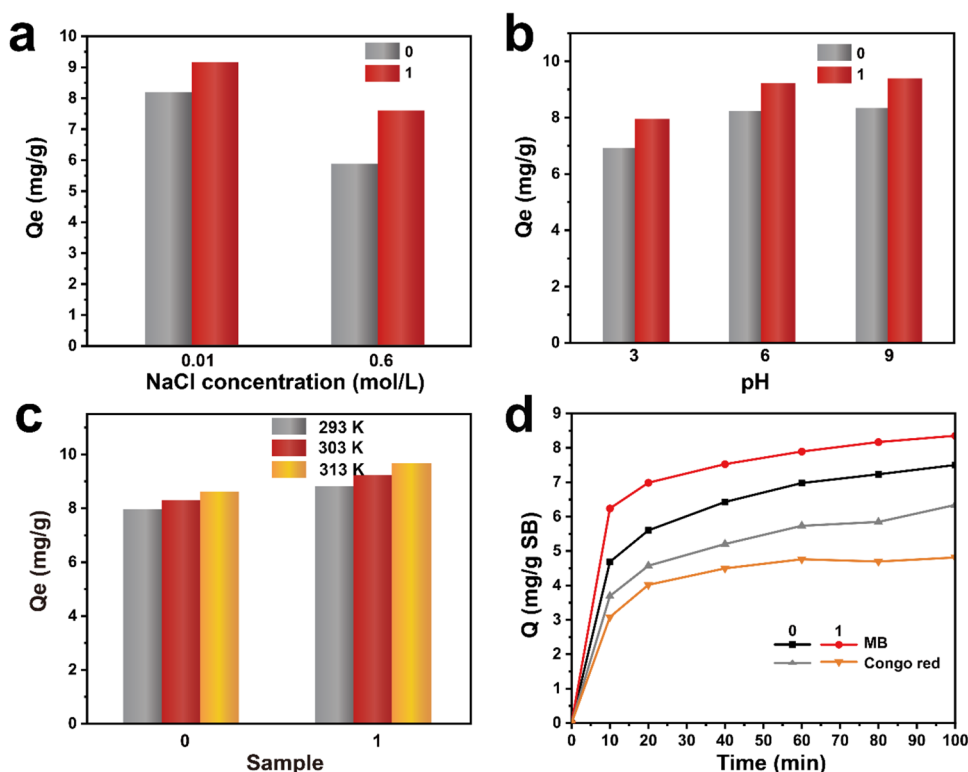
The effects of temperature on the adsorption abilities of SB and ozone-modified SB (Fig. 6c) and the related thermodynamic parameters were also investigated. As shown in Table 9, the $\triangle G^o$ of both SB and ozone-modified SB are both negative, and their absolute values increase with the increasing temperature. This indicated that the adsorption behavior of both SB and ozone-modified SB is spontaneous. The positive value of $\triangle H^o$ indicates that the adsorption process is endothermic. The increase of temperature promotes the increase of adsorption capabilities. Compared to SB, the higher $\triangle H^o$ of SB indicates that it is more sensitive to temperature, and the adsorption capabilities increase higher with the increase of temperature. This is consistent with Fig. 6c. Furthermore, the positive value of $\triangle S^o$ confirms that the endothermic process increases the temperature and thus promotes the movement and randomness of the molecules at the solid/liquid interface.

The adsorption capacity of SB before and after ozone modification to the anionic dye (Congo red) was also compared. As shown in Fig. 6d, SB exhibited higher adsorption capacity for anionic dyes than ozone-modified SB. Compared with MB, the adsorption capacity of SB for Congo red decreased by 15.5%, while that of ozone-modified bagasse decreased by 42.3%. This is strongly related to the increased electrostatic repulsion due to high anionic groups of the ozone-modified SB. This also indicated that the ozone-modified SB exhibited increased sensitivities towards cationic pollutants than SB.

To evaluate the adsorption performance of ozone-modified SB towards cationic polymers with high charges (for example, cationic polyelectrolytes), batch adsorption experiments were conducted by using 0.1-g milled ozone-modified SB to adsorb the 0.001 N cationic PDADMAC. As shown in Fig. 7, the adsorption capability of ozone-modified SB first increased sharply, and then slightly decreased with the increase of the ozone consumption. The adsorption capacity of PDADMAC increased to 125.4% when the ozone consumption was only 1.5 wt% (sample 1). This result was consistent with the change in MB adsorption capacity and the total carboxyl groups. Negatively charged functional groups (carboxyl groups) played an important role during the adsorption of PDADMAC. The increase of negatively charged carboxyl groups on the SB could increase the PDADMAC adsorption because of the existence of chemical reactions or cation exchange between them [54, 55]. Therefore, the increase of carboxyl
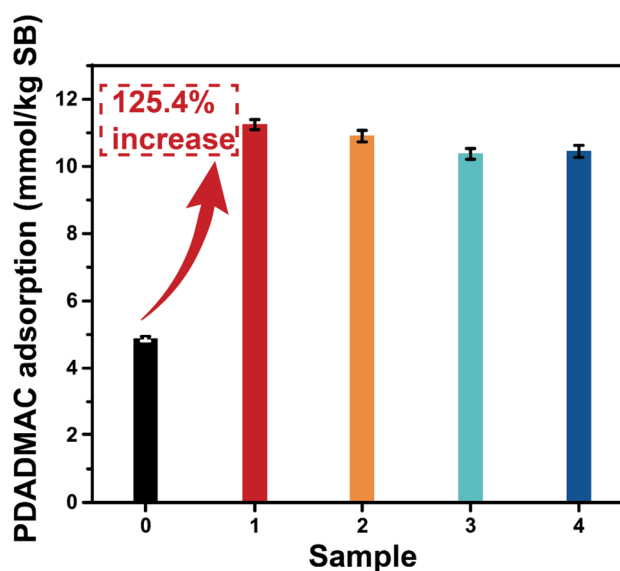

Fig. 7 Adsorption capacity of PDADMAC onto SB and ozone-modified SB with different ozone consumption

groups by ozone modification can effectively increase the PDADMAC adsorption of SB.

4 Conclusion

In this study, SB was successfully modified by ozone at room pressure and temperature. High yield (95.9%), low lignin content (21.9% total lignin removals), and high content of functional groups containing SB were obtained with only 1.5 wt% ozone consumption. The total content of carboxyl groups as the main adsorption sites for cationic organic pollutants was increased by about 84.1%. The increase of the functional groups and reduction of the lignin coverage by ozone modification increased the adsorption abilities of SB. The maximum adsorption rate and equilibrium adsorption capacity of SB for MB were increased by about 33.3% and 11.3%, compared to the original SB (MB concentration = 100 mg/L, SB concentration = 5 g/L, initial solution pH = 6, temperature = 30 °C). Besides, ozone-modified SB maintained its high adsorption capability even at high NaCl concentration (0.6 M). For cationic polymer with high charges (PDADMAC), the adsorption capacity of

Table 9 Thermodynamic parameters for the adsorption of SB and ozone-modified SB	Sample	Initial dye concentration (mg L^{-1})	$\triangle H^o$ (J mol^{-1})	$\triangle S^o$ (J mol^{-1} K^{-1})	$\triangle G^o$ (kJ mol^{-1})		
					293 K	303 K	313 K
	0	100	5.08	0.049	−9.13	−9.61	−10.10
	1	100	6.57	0.055	−9.55	−10.09	−10.65

the milled SB increased about 125.4%. A further increase in the ozone consumption, however, would not increase the adsorption abilities but could decrease the yield. Compared with other modification methods that require high chemical dosage, expensive chemical cost, and high process cost, the amount of ozone used for modification is 15 kg/ton SB (1.5 wt% ozone consumption) with a cost of only US \$72/ton. Besides, ozone-modified SB maintained its high adsorption capability even at a high NaCl concentration of 0.6 M and high pH of 9. Although ozone modification still has a lot of room for improvement in the adsorption capacity of lignocellulosic materials for cationic organic pollutants, considering that ozone is a green and cheap reactant, the combination of ozone modification with other green modification methods could be an industrially feasible and effective way for clean water bodies.

Declarations

Conflict of interest The authors declare no competing interests.

References

1. Guillen J, Natale F, Carvalho N, Casey J, Hofherr J, Druon JN, Fiore G, Gibin M, Zanzi A, Martinsohn JT (2019) Global seafood consumption footprint. Ambio 48(2):111–122

2. Livingstone D, Gallacher S (2003) Contamination and spoilage of molluscs and crustaceans. Encyclopaedia of Food Sciences and Nutrition. Academic Press, Boston, pp 5228–5245

3. Zhou Y, Lu J, Zhou Y, Liu Y (2019) Recent advances for dyes removal using novel adsorbents: a review. Environ Pollut 252:352–365

4. Gupta VK, Ali I, Saleh TA, Nayak A, Agarwal S (2012) Chemical treatment technologies for waste-water recycling—an overview. RSC Adv 2(16):6380–6388

5. Kamran U, Bhatti HN, Iqbal M, Jamil S, Zahid M (2019) Biogenic synthesis, characterization and investigation of photocatalytic and antimicrobial activity of manganese nanoparticles synthesized from Cinnamomum verum bark extract. J Mol Struct 1179:532–539

6. Kamran U, Bhatti HN, Iqbal M, Nazir A (2019) Green synthesis of metal nanoparticles and their applications in different fields: a review. Z Phys Chem 233(9):325–1349

7. Aksu Z (2005) Application of biosorption for the removal of organic pollutants: a review. Process Biochem 40(3–4):997–1026

8. Kamran U, Bhatti HN, Noreen S, Tahir MA, Park SJ (2022) Chemically modified sugarcane bagasse-based biocomposites for efficient removal of acid red 1 dye: kinetics, isotherms, thermodynamics, and desorption studies. Chemosphere 291:132796

9. Schreiber M, Vivekanandhan S, Mohanty AK, Misra M (2012) A study on the electrospinning behaviour and nanofibre morphology of anionically charged lignin. Adv Mat Lett 3:476

10. O'Connell DW, Birkinshaw C, O'Dwyer TF (2008) Heavy metal adsorbents prepared from the modification of cellulose: a review. Bioresour Technol 99(15):6709–6724

11. Pouyet F, Chirat C, Potthast A, Lachenal D (2014) Formation of carbonyl groups on cellulose during ozone treatment of pulp: consequences for pulp bleaching. Carbohyd Polym 109:85–91

12. Wei H, Ma Y, Luo J, Wu KH, Xie W, Wen G, Chiang CL, Yan W, Perathoner S, Centi G, Liu Y (2020) Creation of NC= O active groups on N-doped CNT as an efficient CarboCatalyst for solvent-free aerobic coupling of benzylamine. Carbon 170:338-346

13. Lloyd JA, Horne CW (1993) The determination of fibre charge and acidic groups of radiata pine pulps. Nord Pulp Pap Res J 08(1):048–052

14. Röhrling J, Potthast A, Rosenau T, Lange T, Borgards A, Sixta H, Kosma P (2002) A novel method for the determination of carbonyl groups in cellulosics by fluorescence labeling. 2. Validation and applications. Biomacromolecules 3(5):969–975

15. Liao J, He S, Mo L, Guo S, Luan P, Zhang X, Li J (2021) Mass-production of high-yield and high-strength thermomechanical pulp fibers from plant residues enabled by ozone pretreatment. J Cleaner Prod 296:126575

16. Freudenberg K, Neish AC (1968) Constitution and biosynthesis of lignin. In: Constitution and biosynthesis of lignin. Springer, New York.

17. Kocaefe D, Huang X, Kocaefe Y, Boluk Y (2013) Quantitative characterization of chemical degradation of heat-treated wood surfaces during artificial weathering using XPS. Surf Interface Anal 45(2):639–649

18. Ren JL, Sun RC, Peng F (2008) Carboxymethylation of hemicelluloses isolated from sugarcane bagasse. Polym Degrad Stab 93(4):786–793

19. Laine J, Stenius P, Carlsson G, Ström G (1994) Surface characterization of unbleached kraft pulps by means of ESCA. Cellulose 1(2):145–160

20. Alen R, Andersson R, Annergreen G et al (2011) Chemical pulping Part 1, fibre chemistry and technology. Paper Engineers' Association/Paperi ja Puu Oy, Helsinki.

21. Kamran U, Park SJ (2021) Acetic acid-mediated cellulose-based carbons: influence of activation conditions on textural features and carbon dioxide uptakes. J Colloid Interf Sci 594:745–758

22. Kamran U and Park SJ (2020) MnO2-decorated biochar composites of coconut shell and rice husk: an efficient lithium ions adsorption-desorption performance in aqueous media. Chemosphere 260:127500.

23. Ben H, Chen X, Han G, Shao Y, Jiang W, Pu Y, Ragauskas AJ (2018) Characterization of whole biomasses in pyridine based ionic liquid at low temperature by 31P NMR: an approach to quantitatively measure hydroxyl groups in biomass as their original structures. Front Energy 6:13

24. Mooney CA, Mansfield SD, Touhy MG, Saddler JN (1998) The effect of initial pore volume and lignin content on the enzymatic hydrolysis of softwoods. Bioresour Technol 64(2):113–119

25. Balousek PJ (1979) The effects of ozone upon a lignin-related model compound containing a beta-aryl ether linkage. Lawrence University, Appleton, pp 3–4

26. Pouyet F, Chirat C, Potthast A, Lachenal D (2014) Formation of carbonyl groups on cellulose during ozone treatment of pulp: Consequences for pulp bleaching. Carbohydr Polym 109:85–91

27. Lemeune S, Jameel H, Chang HM, Kadla J (2014) Effects of ozone and chlorine dioxide on the chemical properties of cellulose fibers. J Appl Poly Sci 93(3):1219–1223

28. Abdolali A, Guo W, Ngo HH, Chen SS, Nguyen NC, Tung KL (2014) Typical lignocellulosic wastes and by-products for

biosorption process in water and wastewater treatment: a critical review. Bioresour Technol 160:57–66

29. Gellerstedt F, Gatenholm P (1999) Surface properties of lignocellulosic fibers bearing carboxylic groups. Cellulose 6(2):103–121

30. Zhang Y, Sjögren B, Engstrand P, Htun M (1994) Determination of charged groups in mechanical pulp fibres and their influence on pulp properties. J Wood Chem Technol 14(1):83–102

31. Belgacem M, Czeremuszkin G, Sapieha S, Gandini A (1995) Surface by XPS characterization and inverse gas of cellulose fibres chromatography. Cellulose 2(3):145–157

32. Saha P, Chowdhury S, Gupta S, Kumar I (2010) Insight into adsorption equilibrium, kinetics and thermodynamics of Malachite Green onto clayey soil of Indian origin. Chem Eng J 165(3):874–882

33. Wang H, Yuan X, Zeng G, Leng L, Peng X, Liao K, Peng L, Xiao Z (2014) Removal of malachite green dye from wastewater by different organic acid-modified natural adsorbent: kinetics, equilibriums, mechanisms, practical application, and disposal of dye-loaded adsorbent. Environ Sci Pollutt Res 21(19):11552–11564

34. Salima A, Benaouda B, Noureddine B, Duclaux L (2013) Application of Ulva lactuca and Systoceira stricta algae-based activated carbons to hazardous cationic dyes removal from industrial effluents. Water Res 47(10):3375–3388

35. Ho YS, McKay G (1999) Pseudo-second order model for sorption processes. Process Biochem 34(5):451–465

36. Lagergren SK (1898) About the theory of so-called adsorption of soluble substances. K Sven Vetenskapsakad Hand.

37. Ncibi MC, Mahjoub B, Seffen M (2007) Kinetic and equilibrium studies of methylene blue biosorption by Posidonia oceanica (L.) fibres. J Hazard Mater 139(2):280–285

38. Kumar KV, Sivanesan S, Ramamurthi V (2005) Adsorption of malachite green onto Pithophora sp., a fresh water algae: equilibrium and kinetic modelling. Process Biochem 40(8):2865–2872

39. Vadivelan V, Kumar KV (2005) Equilibrium, kinetics, mechanism, and process design for the sorption of methylene blue onto rice husk. J Colloid Interface Sci 286(1):90–100

40. Aksu Z, Tezer S (2000) Equilibrium and kinetic modelling of biosorption of Remazol Black B by Rhizopus arrhizus in a batch system: effect of temperature. Process Biochem 36(5):431–439

41. Namasivayam C, Kavitha D (2002) Removal of Congo Red from water by adsorption onto activated carbon prepared from coir pith, an agricultural solid waste. Dyes Pigm 54(1):47–58

42. Ho YS (2006) Second-order kinetic model for the sorption of cadmium onto tree fern: a comparison of linear and non-linear methods. Water Res 40(1):119–125

43. Chowdhury S, Saha P (2010) Pseudo-second-order kinetic model for biosorption of methylene blue onto tamarind fruit shell: comparison of linear and nonlinear methods. Bioremediat J 14(4):196–207

44. Dai C, Yang L, Xie J, Wang TJ (2020) Nutrient diffusion control of fertilizer granules coated with a gradient hydrophobic film. Colloids Surf A 588:124361

45. Langmuir I (1918) The adsorption of gases on plane surfaces of glass, mica and platinum. J Am Chem Soc 40(9):1361–1403

46. Freundlich H (1907) Über die adsorption in lösungen. Z Phys Chem 57(1):385–470

47. Redlich O, Peterson DL (1959) A useful adsorption isotherm. Journal of physical chemistry J Phys Chem 63(6):1024–1024

48. Bhattacharyya KG, Sharma A (2005) Kinetics and thermodynamics of methylene blue adsorption on neem (Azadirachta indica) leaf powder. Dyes Pigments 65(1):51–59

49. Kumar KV, Ramamurthi V, Sivanesan S (2005) Modeling the mechanism involved during the sorption of methylene blue onto fly ash. J Colloid Interf Sci 284(1):14–21

50. Wang S, Boyjoo Y, Choueib A, Zhu ZH (2005) Removal of dyes from aqueous solution using fly ash and red mud. Water Res 39(1):129–138

51. Rahman IA, Saad B (2003) Utilization of guava seeds as a source of activated carbon for removal of methylene blue from aqueous solution. Malaysian J Chem 5(1):8–14

52. Vadivelan V, Kumar K (2005) Equilibrium, kinetics, mechanism, and process design for the sorption of methylene blue onto rice husk. J Colloid Interf Sci 286:90–100

53. Luan P, Zhao Y, Li Q, Cao D, Wang Y, Sun X, Liu C, Zhu H (2022) Compressible Ionized Natural 3D interconnected loofah membrane for salinity gradient power generation. Small 18(2):2104320

54. Öner M, Doğan Ö, Öner G (1998) The influence of polyelectrolytes architecture on calcium sulfate dihydrate growth retardation. J Cryst Growth 186(3):427–437

55. Wågberg L (2000) Polyelectrolyte adsorption onto cellulose fibres–a review. Nord Pulp Pap Res J 15(5):586–597

Publisher's note Springer Nature remains neutral with regard to jurisdictional claims in published maps and institutional affiliations.